Eur Respir J, 1995, 8, 1115–1121
DOI: 10.1183/09031936.95.08071115



European Respiratory Journal
ISSN 0903 - 1936

# Quantitative analysis of parenchymal and vascular alterations in $NO_2$-induced lung injury in rats

P.J. Barth*, B. Müller**, U. Wagner**, A. Bittinger*

*Quantitative analysis of parenchymal and vascular alterations in $NO_2$-induced lung injury in rats. P.J. Barth, B. Müller, U. Wagner, A. Bittinger. ©ERS Journals Ltd 1995.*

**ABSTRACT: Nitrogen dioxide ($NO_2$), the oxidation product of nitric oxide (NO), is a reactive free radical forming gas, the inhalation of which has been reported to induce severe damage to distal airways.**

**In order to quantify dose and time course of parenchymal and vascular damage, rats were exposed to 5, 10 and 20 ppm $NO_2$ for 3 and 25 days, followed by quantitative histology and morphometry of the lung.**

**Histological investigations of the short-term exposed animals showed structural alterations extending from slight interstitial oedema after exposure to 5 ppm, to epithelial necrosis and interstitial inflammatory infiltration after exposure to 10 ppm, and an additional intra-alveolar oedema after 20 ppm. The pulmonary arteries disclosed no qualitative changes, such as muscularization of intra-acinar vessels. Long-term exposure to 10 ppm and 20 ppm $NO_2$ resulted in emphysema and slight centrilobular interstitial fibrosis. Morphometric analysis revealed the alveolar surface density to be significantly diminished after short-term exposure to 20 ppm $NO_2$ and long-term exposure to 10 and 20 ppm $NO_2$. The medial thickness of pulmonary arteries was significantly increased after short- and long-term exposure to 20 ppm $NO_2$ and long-term exposure to 10 ppm $NO_2$. In the 5 ppm short- and long-term exposure groups the pulmonary arterial medial thickness was significantly decreased compared to controls. Correlation analysis revealed a negative correlation between average medial thickness and alveolar surface density (coefficient of correlation: -0.56).**

**We conclude that the extent of $NO_2$-induced pulmonary parenchymal and vascular alterations are closely related and concentration- and time-dependent.**

*Eur Respir J., 1995, 8, 1115–1121.*

Depts of *Pathology and **Internal Medicine, Philipps-Universität Marburg/Lahn, Germany.

Correspondence: P.J. Barth
MZ für Pathologie der Philipps-Universität
Baldingerstraβe
35043 Marburg/Lahn
Germany

Keywords: Emphysema
nitrogen dioxide
pulmonary arteries

Received: October 10 1994
Accepted after revision March 25 1995

This study was supported by the Deutsche Forschungsgemeinschaft (Grant No. WA 844/2-1).

Nitrogen dioxide ($NO_2$) - one of the major components of atmospheric air pollution - is a reactive, free radical forming gas. Due to its physicochemical properties, $NO_2$ reaches the lower respiratory tract [1]. Here, it induces dose- and time-dependent parenchymal damage [2]. The structural alterations observed after $NO_2$-exposure can be summarized as diffuse alveolar damage, as described by KATZENSTEIN *et al.* [3]. In the acute phase of $NO_2$-induced diffuse alveolar damage, histological examination discloses epithelial degeneration and necrosis [2, 4–6]. The interstitium and - after exposure to higher doses - the alveolar spaces are filled with an proteinaceous oedema intermixed with polymorphonuclear inflammatory cells. Cellular damage induces consecutive epithelial proliferation and differentiation. Quantitative assessment of the proliferative activity of the airway epithelia revealed the highest proliferative activity in the type II cells; whereas, in the conducting airways the rate of proliferation is lower, decreasing from the distal to the proximal airways [6–8]. The structural and functional alterations, such as increased permeability of endothelium and epithelium, occurring after short-term exposure have been reported to be fully reversible [9]. In humans, short-term exposure to 0.3 ppm $NO_2$ for 30 min has been reported to potentiate exercise-induced bronchospasm in asthmatics [10].

After long-term exposure, emphysema and interstitial fibrosis develop [6, 11]. Therefore, the $NO_2$-induced damage has been proposed as a model for interstitial pneumonia [12]. Nevertheless, as far as we know, vascular changes have not been investigated in $NO_2$ exposed animals. In particular, in most morphological studies the investigators' interest has been focused predominantly on the "parenchymal" and biochemical features of $NO_2$-induced pulmonary damage [13]. Few morphometric studies performed in patients suffering from adult respiratory distress syndrome (ARDS) have reported a close correlation between vascular and parenchymal alterations [14]. As far as we know, no study addressing the question of whether these interactions are reproducible under experimental conditions has so far been published.

Due to its vasodilatatory effect, nitric oxide (NO) is inhalatively applied in patients suffering from severe ARDS with consecutive pulmonary hypertension [15, 16]. Since $NO_2$ results from oxidation of nitric oxide, the question of nitrogen dioxide toxicity gains clinical importance. The therapeutic concentrations of NO range up to 40 ppm for short-term therapy (minutes) and 10–20 ppm for continuous therapy lasting up to several weeks; consecutive $NO_2$ concentrations which have been measured intratracheally and in the expired air have been reported to be lower then 2 ppm [17]. Therefore, $NO_2$-toxicity remains a crucial point to be investigated and safety guidelines have been proposed in order to avoid deleterious effects of $NO_2$ resulting from oxidation of NO [18].

We performed this study in order to analyse the dose- and time-dependence of $NO_2$-induced alterations, with special respect to the morphometric analysis of parenchymal and vascular alterations.

## Materials and methods

For all experiments, specific pathogen-free male Sprague Dawley rats (Charles River Wiga, Sulzfeld, FRG) with 400–450 g body weight were used. A total of 56 animals was subdivided into six exposure groups and two control groups, each comprising seven animals. The exposure groups were exposed to 5, 10 and 20 ppm $NO_2$ for either 3 or 25 days. Controls were exposed in the same way for 3 and 25 days to compressed air.

The animals were kept in cages of four animals with water and food *ad libitum*. The cages were placed into gas-tight chambers equipped with an inlet for a mixture of $NO_2$ and compressed air. A ventilator within the cages was used to produce an equal distribution of the gas atmosphere throughout the box, and a sample port allowed measurements of the actual $NO_2$ concentration. The volume of the exposure boxes was 60 L and the gas flow was adjusted to 15 $L \cdot min^{-1}$ in order to eliminate $CO_2$ from the cage atmosphere. Before the beginning of the experiments, the $NO_2$ concentration within the chambers was controlled every 2 h and corrected if necessary. When the actual $NO_2$ concentration differed less than 5% from the intended value, the animals were put into the cages and the exposure was started. Later, a 6 h determination interval was sufficient to guarantee constance of the $NO_2$-atmosphere within the exposure system. $NO_2$ concentrations were determined using an electrochemical $NO_2$-specific element (ECS 102-1, MPSensor Sytems, 80335 Munich, FRG). For the conditions used in our experiments, the accuracy of this measure has been specified to be 1%. A single gas concentration was the mean of two determinations. During the whole exposure period, the deviation of the $NO_2$-concentration was less than 15% (range) from the intended level.

A weather station was used to control atmospheric pressure, humidity and temperature. As a control, rats were exposed in the same way as described above but only to normal air (sham-exposed animals).

### *Tissue preparation*

After exposure, the animals were anaesthetized by a single intraperitoneal injection of pentobarbital sodium (50 $mg \cdot kg^{-1}$). Whilst the animals were in deep anaesthesia, the lungs and mediastinum were removed *in toto* from the chest cavity. The stem bronchi were cannulated and both lungs were filled with a 4% buffered formaldehyde solution at a constant pressure of 20 $cmH_2O$. Thereafter, the bronchi were ligated, and the lungs were submerged in the fixation solution for at least 12 h. After fixation, the lungs were cut in the frontal plane, the whole tissue was embedded in paraffin, cut at a thickness of 4 µm and stained with haematoxylin and eosin (H&E) and Elastica van Gieson (EvG).

### *Qualitative assessment of the pulmonary arterial vessels*

Arterial vessels were assessed qualitatively with special respect to medial hypertrophy of muscular pulmonary arteries, muscularization of intra-acinar arterioles and cellular intimal proliferation.

### *Morphometry*

In order to quantify the medial size of the muscularized pulmonary arteries the relative medial thickness (RMT) was used. This parameter expresses the thickness of the arterial media as a percentage of the external vessel radius (R) and is well-established for studies aiming at the quantification of dimensional changes of the pulmonary arterial muscularization [6, 14].

Measurements were performed by means of planimetry using a video-linked microscope digitizing board (Ibas I, Zeiss, Kontron, Oberkochen, FRG) as described previously [19]. The method used here is a refined version of that previously described by Cook and Yates [20]; it can also be applied to obliquely and orthogonally cut vessels and requires no prior distension of the vessels, as for example wall-thickness methods. Only those vessels showing a clearly defined internal and external elastic lamina were assessed for medial thickness. In brief, the external (EEL) and internal (IEL) elastic lamina were marked on the screen by means of a light pen. The length of these structures ($L_{IEL}$, $L_{EEL}$) was analyzed together with their major and minor axes by the image analyser. The axes $r_1$ (major axis) and $r_2$ (minor axis) were assessed from the shape circumscribed by the IEL, whereas $R_1$ (major axis) and $R_2$ (minor axis) were analogously derived from the shape of the EEL. In the same procedural step, the area included within the EEL and IEL were measured, from which the medial area (A) was computed (Equation 2.4). External and internal vessel radii were derived from $L_{IEL}$ and $L_{EEL}$ as described by Cook and Yates (Equations (4), (5) and (9)) [19, 20]. The section angle ($\alpha$) at which the vessel is cut can be estimated using Equation (1).

$$\alpha = \arccos(r_1/r_2) = \arccos(R_1/R_2) \quad (1)$$

$$r = L_{IEL}/(\pi*(1.5*(1+\cos^{-1}\alpha)-(\cos^{-1}\alpha)^{1/2}) \quad (2)$$

$$r = L_{IEL}/(2*\pi) = L_{EEL}/(2*\pi) \quad (3)$$

$$A = (A_{EEL}-A_{IEL})*\cos^{-1}\alpha \quad (4)$$

$$T = -r + (r^2 + A/\pi)^{1/2} \quad (5)$$

$$R = r+T \quad (6)$$

$$RMT = (T/R)*100\ (\%) \quad (7)$$

The process of measuring and computation has been described in detail previously, together with the mathematical apparatus [19].

*Computation of the average medial thickness (AMT)*

The average medial thickness (AMT) has been used in order to compare the RMT of vessel populations obtained from several animals. The effort of comparing the data obtained from 56 animals with at least 20 measurements per case by a simple graphic presentation would have led to a scatter plot comprising about 1,120 points. In order to facilitate the comparison, the plots of RMT *versus* R obtained from the different animals AMT values were computed, as described in detail previously [21]. The AMT averages out the RMT for different classes of vessels, which are defined by their R (fig. 1).

In each animal, at least 20 vessels with R of 40–160 µm were assessed for R and RMT as described above. In brief, the RMT was plotted against the corresponding R (fig. 1). This scatterplot was fitted to a curve of the common form ($RMT=a*R^b$; where a and b=constants) by means of least square regression and the coefficient of correlation was computed. For all cases measured in this study, correlation coefficients were found to be less than -0.55 ($p<0.05$) with a median value of -0.79 ($p<0.05$). With the curve obtained from curve fitting, the AMT of vessels with a defined R was then computed in an interval ($I_i$: $g \leq R \leq h$) according to [21]:

$$AMT(I_i) = \int_g^h a*R^b\, dR \quad (8)$$

In the present study we chose four intervals ($I_1$: 40 µm≤R≤70 µm; $I_2$: 70 µm≤R≤100 µm; $I_3$: 100 µm≤130 µm; $I_4$: 130 µm≤R≤160 µm) for the computation of AMT-values (fig. 1).

*Assessment of alveolar surface density*

The alveolar surface density ($S_{v(Alv)}$) was stereologically assessed using a rectangular ocular test grid (Periplan 10× M, Leitz, Wetzlar, FRG). The number of intersections (k) between test grid lines and alveolar septae was counted at 160× microscopic magnification. With known test line length (L) the alveolar surface density can be computed according to [22]:

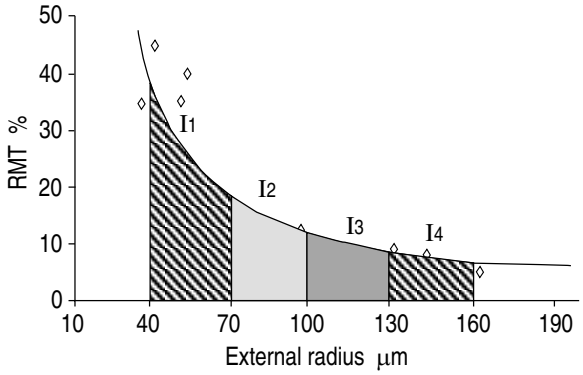


Fig. 1. – The different intervals ($I_1$–$I_4$) in which the average medial thickness (AMT) was computed for each animal. RMT: relative medial thickness.

$$S_{v(Alv)} = \frac{2\times\Sigma k}{L} \quad (\mu m^{-1}) \quad (9)$$

The dimension of $S_{v(Alv)}$ is $\mu m^{-1}$ and is, therefore, equivalent to the alveolar surface per unit lung volume ($\mu m^{-1} = \mu m^2/\mu m^3$). Reduction of $S_{v(Alv)}$ is related to an increasing degree of emphysema. The correlation between $S_{v(Alv)}$ and the mean linear intercept (MLI), which has also been used as a measure for emphysema [23]; is approximately: $S_{v(Alv)}=2/MLI$. In each animal, at least 40 measuring fields were assessed, the standard error of measurements was less than 10%.

*Statistical analyses*

Normal distribution of group values was confirmed using the Kolmogoroff-Smirnoff test. For normally distributed data, differences between multiple groups were tested for statistical significance using the multiple variance procedure; pairwise testing was performed using the Scheffé test. In the figures, normally distributed data are represented by their arithmetic mean±standard deviation. Statistical significance of differences between multiple groups which were not normally distributed was tested using the Kruskall-Wallis H-test. Pairwise comparison of two groups was performed according to the Mann-Whitney U-test after Bonferoni's adjustment of the p-levels. The data of these groups are characterized by median values. Correlation analysis and curve fitting were performed according to the method of least sum of squared errors. The computation of the correlation between alveolar surface density and average medial thickness (fig. 2, table 1) is based on 56 values (7 animals × 6 exposure groups + 7 animals × 2 control groups).

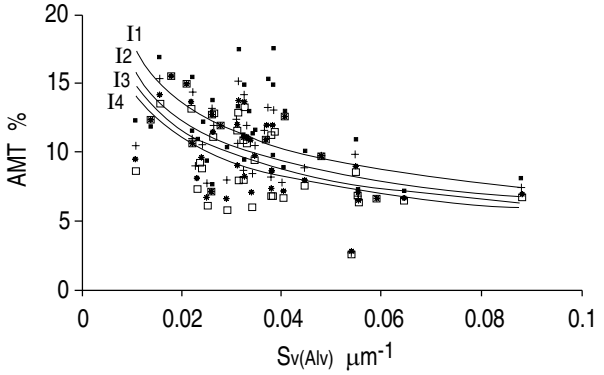


Fig. 2. – Plot of alveolar surface density ($S_{v(Alv)}$) *versus* average medial thickness (AMT) of the different vessel populations ($I_1$–$I_4$) together with regression curve. With decreasing $S_{v(Alv)}$ (*i.e.* increasing degree of emphysema) the AMT increases. ■ : AMT($I_1$); +: AMT($I_2$); *: AMT($I_3$); ❑ : AMT($I_4$). The computation of each regression curve is based on 56 values (7 animals × 6 exposure groups + 7 animals × 2 control groups).

Table 1. – Correlation coefficients (r) and constants (a and b) for: $AMT(I_n)=a*S_{v(Alv)}^b$

| Interval | r | a | b | p- value | n |
|---|---|---|---|---|---|
| $I_1$ | -0.56 | 2.97 | -0.40 | 0.01 | 56 |
| $I_2$ | -0.65 | 2.20 | -0.45 | 0.01 | 56 |
| $I_3$ | -0.65 | 1.82 | -0.49 | 0.05 | 56 |
| $I_4$ | -0.64 | 1.57 | -0.52 | 0.05 | 56 |

AMT: average medial thickness; $I_n$: interval of computation; $S_{v(Alv)}$: alveolar surface density.

## Results

### *Qualitative histological investigations*

After short-term exposure to 5 ppm $NO_2$, the lung tissue histologically revealed a slight interstitial oedema, epithelial necrosis or degeneration were not confirmed by means of light microscopy. Short-term exposure to 10 ppm $NO_2$ resulted in an interstitial oedema and dense interstitial polymorphomononuclear infiltration, predominantly in the interstitium of the respiratory bronchioles and the centroacinar alveolar septae. The alveolar spaces appeared to be of normal dimension. The bronchiolar epithelium showed necrosis and its surface was covered with cellular debris. After short-term exposure to 20 ppm $NO_2$ the morphological changes described were more severe and the centroacinar alveoli were filled with an intra-alveolar oedema intermixed with inflammatory cells and cellular debris. The epithelium of the respiratory bronchioles, and to a lesser extent terminal bronchioli, showed extensive necrosis.

After long-term exposure, animals exposed to 5 ppm showed no significant qualitative changes of the lung tissue. Long-term exposure to 10 and 20 ppm $NO_2$ resulted in slight fibrosis of the centroacinar alveolar septa and respiratory bronchioli. In both exposure groups, the lumen of terminal and respiratory bronchioli was, in part, occluded by fibrous cuffs. The alveolar spaces appeared to be irregularly shaped and the interstitium disclosed slight fibrosis (fig. 3).

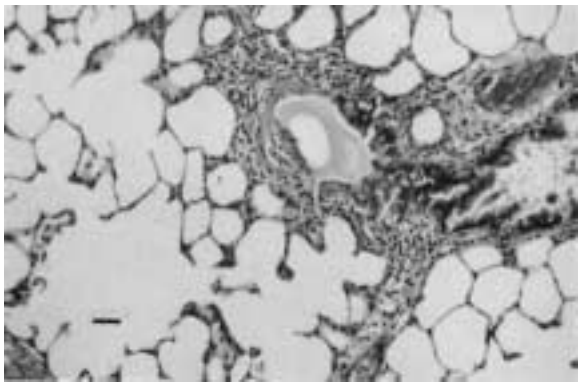

Fig. 3. – Microphotograph of lung tissue after exposure to 10 ppm $NO_2$ for 25 days. The bronchiolar walls are thickened and show a slight inflammatory infiltration. Centroacinar alveolar spaces are irregularly shaped and distended. (Internal scale bar=30 µm).

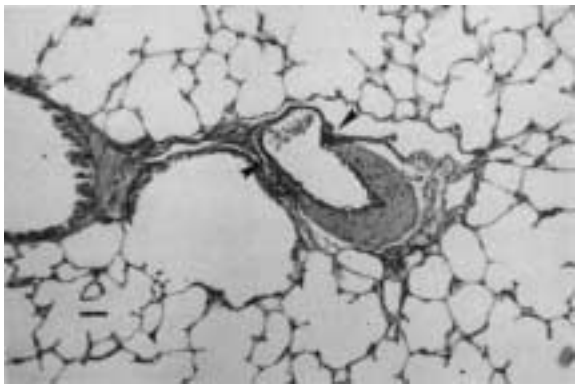

Fig. 4. – Microphotograph showing the abrupt transition of a preacinar muscularized artery into a partially muscularized intra-acinar arteriole (arrowheads). The concomitant bronchiole can be seen on the left side. (Internal scale bar=30 µm).

Qualitative changes of the pulmonary arteries or arterioles could not be confirmed by light microscopy; in particular, no muscularization of intra-acinar arteries was found. Also, hyaline, necrotic or arteritic changes of the vessels were not detected. Figure 4 shows the transition of an preacinar muscular artery into an intra-acinar non-muscularized vessel.

### *Morphometry*

*Emphysema.* In control animals, the alveolar surface density was 0.044±0.010 $\mu m^{-1}$. After 5 ppm exposure, no significant difference was found in the short-term (0.056±0.017 $\mu m^{-1}$) and long-term (0.052±0.009 $\mu m^{-1}$) exposure groups. Short-term exposure to 10 ppm (0.048±0.016 $\mu m^{-1}$) did also not result in a significant change of the alveolar surface density. After long-term exposure to 10 ppm $NO_2$ the alveolar surface density decreased to a value of 0.032±0.006 $\mu m^{-1}$. This extent of decrease in alveolar surface density had already been observed in the 20 ppm short-term exposure group (0.028±0.008 $\mu m^{-1}$). Long-term exposure to this concentration (0.028±0.011 $\mu m^{-1}$) did not result in a further decrease of the alveolar surface density (fig. 5).

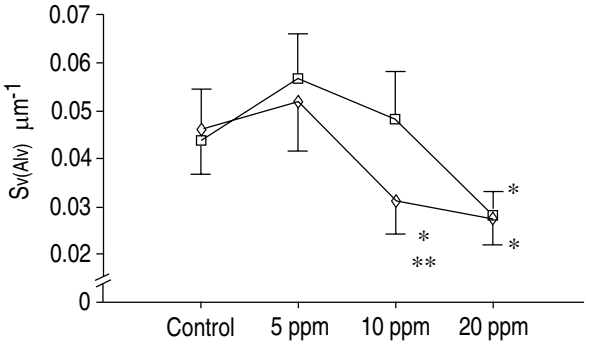


Fig. 5. – Exposure dose- and time-dependence of the alveolar surface density ($S_{v(Alv)}$). Group values are represented by mean±standard deviations. □: 3 day exposure (short); ◊: 25 day exposure (long). *: $p<0.05$ for significant difference between group value and controls; **: $p<0.05$ for significant difference between short- and long-term exposure groups.

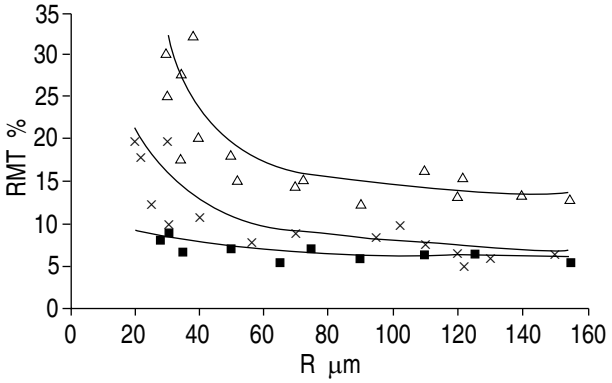


Fig. 6. – Plot of relative medial thickness (RMT) *versus* external radius (R) together with regression curves of one control animal (×), one animal exposed to 20 ppm $NO_2$ for 25 days (Δ) and one animal exposed to 5 ppm NO for 3 days (■).

*Quantitative assessment of pulmonary arterial thickness*

The RMT of unexposed control animals was about 20% for vessels with an R of 40 µm; between 40–70 µm the RMT rapidly decreased with rising R, thereafter, for R ≥70 µm the RMT decreased only slightly to values of about 8%. The AMT in consequence decreased from $I_1$ to $I_2$, $I_3$ and $I_4$.

Figure 6 depicts characteristic plots of RMT *versus* R of one control animal, together with the data obtained from two exposed animals. All exposure groups showed a similar course of the regression curves. The highest RMT values were measured in the 20 ppm long-term exposure group, whereas in the 5 ppm short-term exposure group significantly lower values, even lower than those of the control group were found.

*Computation of average medial thickness (AMT)*

The AMT values of exposure and control groups are depicted in figure 7. After short-term exposure to 10 ppm $NO_2$ no significant change of the AMT was observed, whereas after short-term exposure to 20 ppm all vessel populations ($I_1$–$I_4$) investigated showed a significantly increased AMT. Animals exposed to 5 ppm $NO_2$

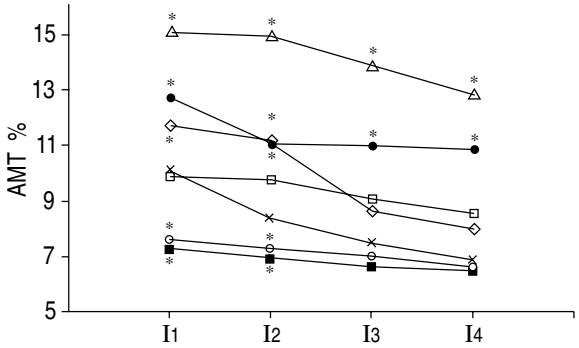


Fig. 7. – Average medial thickness (AMT) in the different exposure groups and investigated intervals. Group values are represented by the median. —Δ— : 20 ppm 25 day; —●— : 20 ppm 3 day; —□— : 10 ppm 3 day; —◇—: 10 ppm 25 day; —×— : control; —○— : 5 ppm 25 day; —■— : 5 ppm 3 day. *: $p<0.05$ between exposure group and controls of the corresponding interval.

disclosed a significantly lower AMT in vessels with an R lower than 100 µm; AMT of larger vessels did not significantly differ from controls.

After long-term exposure to 20 ppm $NO_2$ the AMT was significantly higher compared to controls in all vessel classes ($I_1$–$I_4$) investigated. The 10 ppm exposure disclosed a significant increase of the AMT for vessels with R of 40–100 µm ($I_1$–$I_2$), whereas larger vessels showed no significant change in AMT compared to controls.

As already observed in the short-term exposure group, the 5 ppm long-term exposure resulted in a significant decrease of the AMT for vessels with R smaller than 100 µm ($I_1$–$I_2$).

*Correlation between alveolar surface density and average medial thickness*

Figure 2 depicts a plot of AMT *versus* ($S_{v(Alv)}$) together with the corresponding regression curves obtained for the four vessel populations ($I_{1–4}$) investigated. The correlation coefficients and constants a and b are listed in table 1. The plots $S_{v(Alv)}$ *versus* AMT (fig. 2) together with the regression curves for the intervals ($I_{1–4}$) investigated disclose an inverse correlation between AMT and $S_{v(Alv)}$.

## Discussion

The present study was performed in order to investigate the dose- and time-dependence of parenchymal and vascular changes induced by inhaled $NO_2$. The qualitative and morphometric data obtained in this study suggest three different patterns of structural reaction to inhaled $NO_2$. These are influenced mainly by the dose and duration of exposure. Exposure to low (≤5 ppm) doses resulted in a slight interstitial oedema, qualitative vascular changes were not observed in these exposure groups; whereas, a significant decrease in average medial thickness was detected for arteries with an external radius of

less than 100 μm. Doses of 10 ppm $NO_2$ induce parenchymal and vascular alterations after long-term exposure, whereas short-term exposure is not related to emphysema or medial hypertrophy. This fact is obviously due to a concentration × time (C×T)-dependence of both the structural alterations. For 20 ppm $NO_2$, acute toxicity must be postulated. Even after short-term exposure, this concentration leads to severe parenchymal damage that can be attributed to the breakdown of the enzymatic antioxidant system of the lung, which is mostly composed of the glucose-6-phosphate-dehydrogenase, glutathione reductase, glutathione oxidase and superoxide dismutase, as described by several authors [24, 25]. In contrast to the consecutive $NO_2$-induced epithelial damage, which is primarily due to radical formation and consecutive lipid peroxidation [1, 2], $NO_2$-induced emphysema is caused by an acute imbalance of the pulmonary protease anti-protease system [26]. $NO_2$, in part, directly affects the protein structure of the $\alpha_1$-proteinase inhibitor ($\alpha_1$-PI) leading to reduction of the specific activity of the enzyme [27], and secondly leads to the release of proteolytic enzymes from inflammatory cells [28].

Although the correlation between pulmonary hypertension and emphysema is well-documented and analysed on clinical and pathophysiological levels, structural analyses of these features have rarely been performed in experimental pathology [23, 29]. Earlier publications suggest the capillary and alveolar surface density to be directly correlated [22]. We therefore assume the diminution of the pulmonary capillary network to be reflected by the reduction of the alveolar surface density. The data described in this paper clearly demonstrate that medial hypertrophy of the pulmonary arteries - especially in the early stages of pulmonary hypertension - primarily affects the smallest, fully muscularized preacinar arteries (40 μm≤R≤100 μm); whereas, hypertrophy of larger arteries is found in the consecutive stages of disease. In the setting of this study, qualitative changes of partially muscularized intra-acinar arteries and arterioles could not be confirmed.

The methodology described here proves to be a sensitive tool for the assessment of changes in medial dimension in different subpopulations of the pulmonary arteries. Planimetric measurements enable the investigator to detect significant quantitative changes of the pulmonary arterial vasculature before qualitative changes, as for example muscularization of intra-acinar arteries occurs. A striking phenomenon is the decrease of average me dial thickness in the 5 ppm exposure groups. The methodology used in this study is a refined version of that originally devised by Cook and Yates [20], who reported this method to be independent of the state of constriction or dilatation of the vessel measured. The significant decrease in average medial thickness is, therefore, not a result of vasodilatation, it rather reflects the reduction in pulmonary arterial muscle mass. Such a rapid reduction of pulmonary arterial muscularization can also be observed as a sequel of diminished pulmonary arterial pressures occurring during intrauterine pulmonary maturation and transition to extrauterine life [30, 31]. In our experimental setting, it remains unclear whether $NO_2$ itself exerts a vasodilatatory effect or if this effect has to be attributed to nitric oxide (NO). NO, which has been reported to be a potent dilatator of the pulmonary vascular bed [15–17], and nitrate result from disproportionation of $NO_2$ in aqueous solutions, and the NO/haeme protein complex has been detected under experimental conditions quite similar to those applied in the present study [32].

One must assume that, even with higher doses, inhaled $NO_2$-induced morphological alterations of the pulmonary arteries are ameliorated by vasodilatation. From this we conclude that in other experimental models, with similar degrees of emphysema, medial hypertrophy might be more extreme. The dilatatory effect on the pulmonary vasculature has, therefore, always to be considered when analyses on the pulmonary arteries are performed in $NO_2$ exposed animals.

***Acknowledgements***: The authors thank S. Koch, F. Schwarz and A. Wächtershäuser for their skilful technical assistance.

## References

1. Morrow PE. Toxicological data on $NO_2$: an overview. *J Toxicol Environ Health* 1984; 13: 205–227.
2. Bils RF, Christie BR. The experimental pathology of oxidant and air pollutant inhalation. *Int Rev Exp Pathol* 1980; 21: 195–293.
3. Katzenstein AA, Bloor CM, Liebow AA. Diffuse alveolar damage: the role of oxygen, shock and related factors. *Am J Pathol* 1976; 85: 210–218.
4. Case BW, Gordon RE, Kleinerman J. Acute bronchiolar injury following nitrogen dioxide exposure: a freeze fracture study. *Environ Res* 1982; 29: 399–413.
5. Kawakami M, Yasui S, Yamawaki I, Katayama M, Nagai A, Takizawa T. Structural changes in airways of rats exposed to nitrogen dioxide intermittently for seven days. *Am Rev Respir Dis* 1989; 140: 1754–1762.
6. Barth PJ, Uhlarik S, Bittinger A, Wagner U, Rüschoff J. Diffuse alveolar damage in the rat lung after short- and long-term exposure to nitrogen dioxide. *Path Res Pract* 1994; 190: 33–41.
7. Barth PJ, Müller B, Wagner U, Bittinger A. Assessment of proliferative activity in type II pneumocytes after inhalation of $NO_2$ by AgNOR analysis. *Exp Toxic Pathol* 1994; 46: 335–342.
8. Barth PJ, Wagner U, Bittinger A, Müller B. Topologic analysis of cell renewal after $NO_2$ inhalation in rats by AgNOR analysis. *In*: Müller B, von Wichert P, eds. Lung Surfactant: Basic Research in the Pathogenesis of Lung Disorders. Basel, Karger, 1994; pp. 169–173.
9. Man SFP, Williams DJ, Amy RA, Man GCW, Lien DC. Sequential changes in canine pulmonary epithelial and endothelial cell functions after nitrogen dioxide. *Am Rev Respir Dis* 1990; 142: 199–205.
10. Bauer MA, Utell MJ, Morrow PE, Speers DM, Gibb FR. Inhalation of 0.30 ppm nitrogen dioxide potentiates exercise-induced bronchospasm in asthmatics. *Am Rev Respir Dis* 1986; 134: 1203–1208.
11. Juhos LT, Green DP, Furiosi NJ, Freeman G. A quantitative study of stenosis in the respiratory bronchiole of the rat in $NO_2$-induced emphysema. *Am Rev Respir Dis* 1980; 120: 541–549.
12. Last JA, Gelzleichter TR, Pinkerton KE, Walker RM,

Witschi H. A new model of progressive pulmonary fibrosis in rats. *Am Rev Respir Dis* 1993; 148: 487–494.
13. Müller B, Barth P, von Wichert P. Structural and functional impairment of surfactant protein A after exposure to nitrogen dioxide in rats. *Am J Physiol (Lung Cell Mol Physiol 7)* 1992; 263: L177–L184.
14. Barth PJ, Knoch M, Müller E, Sangmeister C, Bittinger A. Morphometry of parenchymal and vascular alterations in ARDS after extracorporal carbon dioxide removal therapy ($ECCO_2$-R-therapy). *Path Res Pract* 1994; 188: 653–656.
15. Rossaint R, Falke KJ, López F, Slama K, Pison U, Zapol WM. Inhaled nitric oxide for the adult respiratory distress syndrome. *N Engl J Med* 1993; 328: 399–405.
16. Pepke-Zaba J, Higenbottom TW, Dingh Xuan AT, Stone D, Wallwork J. Inhaled nitric oxide as a cause of selective pulmonary vasodilatation in pulmonary hypertension. *Lancet* 1991; 338: 1173–1174.
17. Girard C, Lehot JJ, Pannetier JC, Filley S, Ffrench P, Estanove S. Inhaled nitric oxide after mitral valve replacement in patients with chronic pulmonary artery hypertension. *Anesthesiology* 1992; 77: 880–883.
18. Foubert L, Fleming B, Latimer R, *et al*. Safety guidelines for use of nitric oxide. *Lancet* 1992; 339: 1615–1616.
19. Barth PJ, Kimpel Ch, Roy S, Wagner U. An improved mathematical approach for the assessment of the medial thickness of pulmonary arteries. *Path Res Pract* 1993; 189: 567–576.
20. Cook TA, Yates PO. A critical survey of techniques for arterial mensuration. *J Path* 1972; 108: 119–127.
21. Barth PJ, Rüschoff J. Morphometric study on pulmonary arterial thickness in pulmonary hypoplasia. *Pediatr Pathol* 1992; 12: 653–663.
22. Weibel ER. Morphometry: stereological theory and practical methods. *In*: Gil J, ed. Models of Lung Disease: Microscopy and Structural Methods. New York, Marcel Dekker, 1990.
23. Lay YL, Olson JW, Gillespie MN. Ventilatory dysfunction precedes pulmonary vascular changes in monocrotaline-treated rats. *J Appl Physiol* 1991; 70: 561–566.
24. Menzel DB. Antioxidant vitamins and prevention of lung disease. *Ann NY Acad Sci* 1992; 669: 141–155.
25. Sagai M, Ichinose T, Oda H, Kubota K. Studies on biochemical effects of nitrogen dioxide. II. Changes of the protective systems in rat lungs and of lipid peroxidation by acute exposure. *J Toxicol Environ Health* 1982; 9: 153–164.
26. Kleinerman J, Ip MPC, Sorensen J. Nitrogen dioxide exposure and alveolar macrophage elastase in hamsters. *Am Rev Respir Dis* 1982; 125: 203–207.
27. Hood DB, Gettins P, Johnson DA. Nitrogen dioxide reactivity with proteins: effects on activity and immunoreactivity with $alpha_1$-proteinase inhibitor and implications for $NO_2$-mediated peptide degradation. *Arch Biochem Biophys* 1993; 304: 17–26.
28. Guth DJ, Mavis RD. Biochemical assessment of acute nitrogen dioxide toxicity in rat lung. *Toxicol Appl Pharmacol* 1985; 81: 128–138.
29. Snow RL, Davies P, Pontoppidan H, Zapol WM, Reid L. Pulmonary vascular remodeling in adult respiratory distress syndrome. *Am Rev Respir Dis* 1982; 126: 887–892.
30. Reid LM. Lung growth in health and disease. *Br J Dis Chest* 1984; 78: 113–134.
31. Davies G, Reid L. Growth of the alveoli and pulmonary arteries in childhood. *Thorax* 1975; 25: 669–681.
32. Maples KR, Sandstrom T, Su YF, Henderson RF. The nitric oxide/heme protein complex as a biologic marker of exposure to nitrogen dioxide in humans, rats, and *in vitro* models. *Am J Respir Cell Mol Biol* 1991; 4: 538–543.